

**Yanhui Zhao**

e-mail: yzz127@psu.edu

**Thomas Walker**

e-mail: stesichorus@gmail.com

**Yue Bing Zheng**

e-mail: yzz113@gmail.com

**Sz-Chin Steven Lin**

e-mail: ssl130@psu.edu

**Ahmad Ahsan Nawaz**

e-mail: aan141@psu.edu

**Brian Kiraly**

e-mail: btk5051@psu.edu

**Jason Scott**

e-mail: jms6824@psu.edu

**Tony Jun Huang**

e-mail: junhuang@psu.edu

Department of Engineering Science  
and Mechanics,  
The Pennsylvania State University,  
University Park, PA 16802

# Mechanically Tuning the Localized Surface Plasmon Resonances of Gold Nanostructure Arrays

*We report the fabrication of metal nanostructures on a polydimethylsiloxane (PDMS) substrate by transferring polystyrene beads onto PDMS substrate followed by metal deposition. Experimentally tuning the plasmon resonance of the metal nanostructures was demonstrated by stretching the patterned PDMS substrate. The distance between adjacent nanodisks affects the coupling between the disks, leading to a repeatable and reversible shift in the spectrum. The device can be valuable in many applications such as biochemical sensing, reconfigurable optics, and the study of coupled resonances.*

[DOI: 10.1115/1.4006616]

## 1 Introduction

Plasmonics integrates electromagnetic waves with metal nanostructures, allowing the manipulation of electromagnetic waves at the nanometer scale [1,2]. This provides the possibility for all-optical, ultrahigh-speed computing or even the creation of networks and grids with much faster speeds and lower energy losses compared to current microelectronic circuits [3–10]. It also provides a means to circumvent optical diffraction limits—which restrict the image resolution of the microscope—via the use of various metamaterials such as the superlens [11,12], hyperlens [13,14], and their derivatives [15,16]. Active metamaterials consisting of both metal structures and an active medium such as liquid crystals [17–24] or bistable molecules [25–34] have also been demonstrated as effective nanoscale optical modulators. Advanced fabrication techniques have equipped researchers with a powerful toolkit to further explore plasmonic phenomena [35–39].

Localized surface plasmon resonance (LSPR) [40,41] is an important branch of plasmonics, linking metal nanoparticles with extraordinary optical responses. LSPR occurs when the oscillating frequency of incident light matches with the intrinsic electron resonance on the surface of a noble metal nanoparticle. Enhanced electron oscillations at the resonance frequency cause increased optical absorption, thus LSPR is characterized by peaks in the absorption spectrum. The factors affecting LSPR include the size and shape of particles/holes [42,43], the distance between adjacent particles/holes, the thickness of the fabricated structures, and the environment surrounding the structures [44–50]. Specific LSPR peaks can be obtained by engineering the metal nanostructures into different sizes and arrangements [51]. However, for each desired LSPR, a different corresponding geometry must be designed and fabricated. Active plasmonics that can actively tune

the LSPR after fabrication via flexible approaches utilizing either mechanical stretching or thermal expansion to alter the nanostructure substrate possesses a highly desirable feature preferred in applications such as plasmonic switches or biosensing [52–54].

Here, we describe a method to fabricate Au nanodisks onto an elastic PDMS substrate. Due to the weak bonding between Au and PDMS, the nanostructures were fabricated onto an intermediate layer for sufficient adhesion. In addition, by mechanically stretching the PDMS substrate, above which sit the Au-patterned nanostructures, we observed a real-time tuning of the plasmonic resonance due to the varying distance between adjacent nanodisks. Our design utilizes low-cost nanofabrication techniques and can find application in plasmonic sensing [55], optical imaging, optical memory elements, and energy harvesting [56].

## 2 Experimental Details

A schematic of the working mechanism is shown in Fig. 1. In order to dynamically tune the LSPR of an Au nanostructure array, we fabricated the array on the resilient, mechanically limber substrate: PDMS. However, the deposition of Au directly on PDMS is not favorable as the two only weakly interact. To overcome this challenge, we used a monolayer self-assembly process based on a standard Langmuir–Blodgett [57] followed by standard etching and film deposition procedures.

The PDMS substrate was prepared as follows: First, a silicon wafer with smooth surfaces was cleaned and coated with 1H, 1H, 2H, 2H-perfluorooctyltrichlorosilane (Sigma-Aldrich) to reduce the surface energy. This treatment protects the PDMS from deformation during the detachment process and significantly reduces the surface roughness. Next, Sylgard® 184 Silicone Elastomer base and curing agent (Dow Corning, Midland, MI) were mixed in a 10:1 weight ratio and applied to the pretreated silicon wafer. The mixture was then cured at 70 °C for 20 min. Once cured, it was cut and peeled from the silicon wafer. Finally, a zapping

Manuscript received September 16, 2011; final manuscript received February 8, 2012; published online August 13, 2012. Assoc. Editor: Henry Hess.

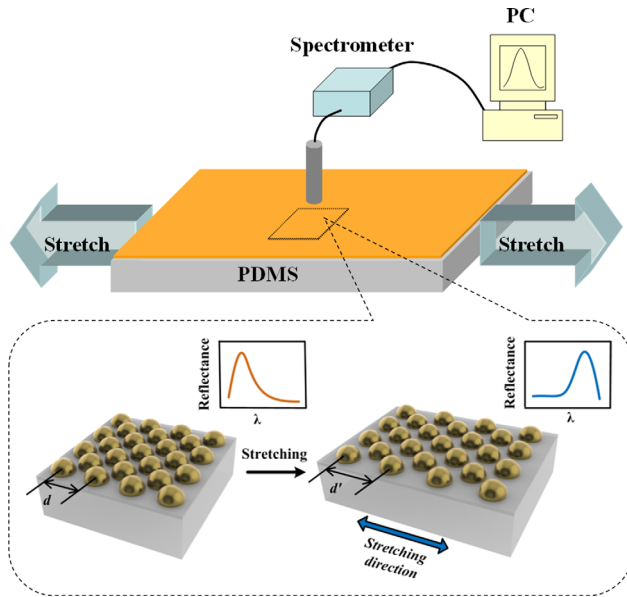


**Fig. 1 Schematic of the experimental setup. The active tuning of LSPR of the Au nanodisk arrays is achieved by mechanically stretching the sample.**

process was initiated to create charges on the PDMS surfaces to increase the bonding between PDMS and dielectric materials.

Polystyrene (PS) nanospheres with a mean diameter of  $1.05\ \mu\text{m}$  were obtained in solution (10 wt. %; Bangs Laboratories, Inc.) and diluted to 1 wt. % with ethanol. The diluted suspension was pulled into a pre-cleaned Langmuir–Blodgett deposition trough (KSV NIMA) filled with deionized water. Upon the addition of several

microliters of sodium dodecyl sulfate, the PS nanospheres were dispersed on the water surface (Fig. 2(a)). The barriers of the trough were brought close together to form a monolayer of PS nanospheres (Fig. 2(b)). The PDMS slab was then placed onto the patterned monolayer to directly transfer the PS nanosphere array from the liquid surface to the pretreated PDMS surface (Figs. 2(c) and 2(d)). A plasma etching process was applied to flatten and separate the transferred PS nanospheres. As shown in Fig. 2(g), the diameter of the PS nanospheres shrinks from  $1.05\ \mu\text{m}$  to  $800\ \text{nm}$  after etching, leaving the spacing between adjacent nanospheres around  $250\ \text{nm}$ . Finally, a 2-nm-thick adhesion layer of Cr and a 40-nm-thick layer of Au were sputtered onto the reshaped nanospheres to form the Au nanostructure arrays. Figure 2(h) shows the SEM image of the sample after Cr/Au deposition. The hexagonal array has a period of  $1.05\ \mu\text{m}$  and a spacing of  $\sim 165\ \text{nm}$ . The observed structures are nanonipple-like structures rather than in perfect disk shapes because the beads supporters would not provide a flat surface for the deposition after etching. However, it does not affect our concept of plasmonic tuning via PDMS substrate stretching, and the shape effect on plasmonic resonance is not the focus of our work. Thus, we approximated the nanonipples to nanodisks for the simplicity of simulation and analysis, and our approximation has been confirmed and supported in both simulation and experiment.

The experimental setup is schematically illustrated in Fig. 1. The dimension of sample we used in the experiment is around  $1\ \text{cm}$  by  $1\ \text{cm}$ , cutting from a large sample area. The sample was affixed to a caliper with a stretching range of  $0$  to  $2000\ \mu\text{m}$  and a precision of  $10\ \mu\text{m}$ . An ultraviolet-visible-infrared spectrometer (Ocean Optics Co., HR4000) was operated in reflection mode to measure the reflectance spectrum of the Au nanostructure arrays. Both the source and detector optical fibers were mounted normal to the sample. The dynamic tuning of LSPRs from Au nanostructure arrays was then monitored over a spectral range of  $400$ – $900\ \text{nm}$  upon sample stretching.

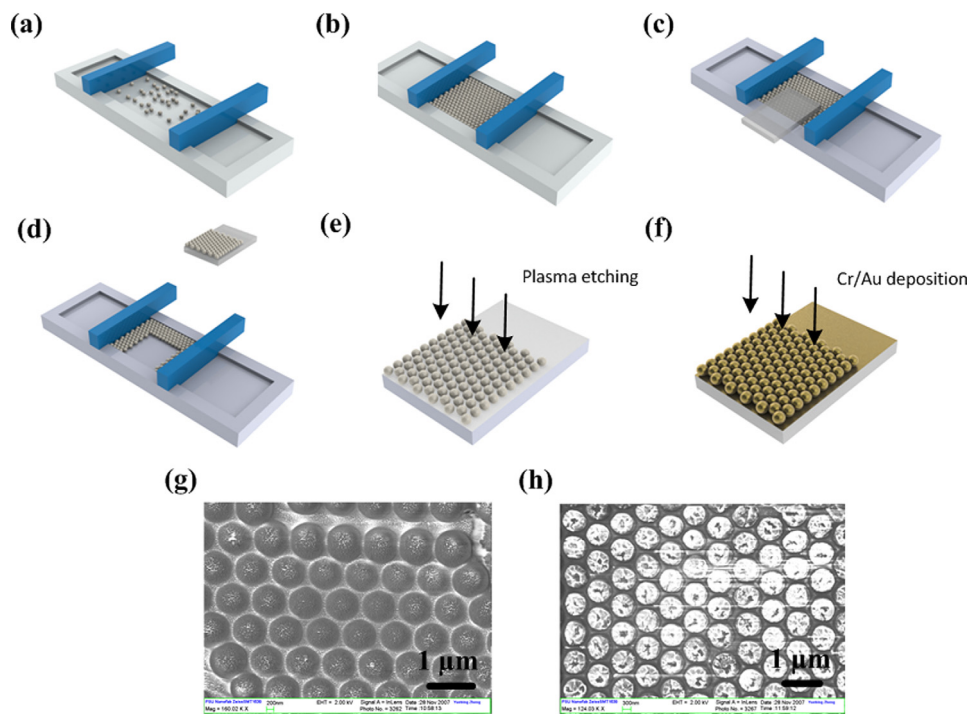


**Fig. 2 Procedures of fabricating Au nanostructure arrays on a PDMS substrate using the Langmuir–Blodgett technique, deposition, and etching. (a) Disperse PS nanospheres in DI water. (b) Compress the squeeze bars to form a compact monolayer of PS nanospheres. (c) Attach a smooth PDMS substrate to the monolayer of nanospheres. (d) The bonding force between PS nanospheres and PDMS substrate helps to transfer the nanosphere arrays onto the surface of PDMS substrate. (e) Reshape nanospheres using plasma etching. (f) Deposit Cr/Au on top of the nanosphere arrays. SEM images of the sample after step (e) and (f) are shown in (g) and (h), respectively.**

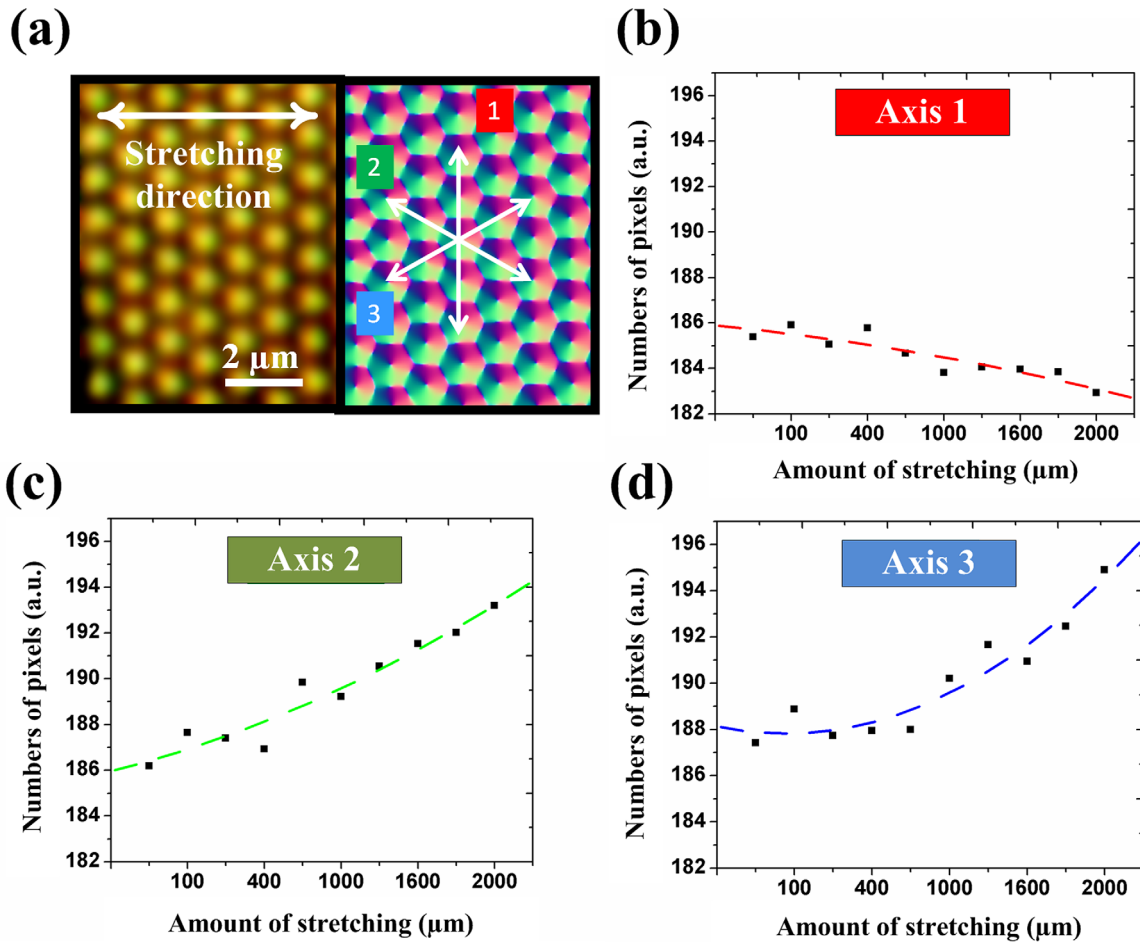


Fig. 3 (a) Microscopic image of Au nanodisk array immobilized on a PDMS substrate. Three axes of the hexagonal array are marked for measuring the geometry change upon stretching. (b)–(d) The measured change in array period along three axes.

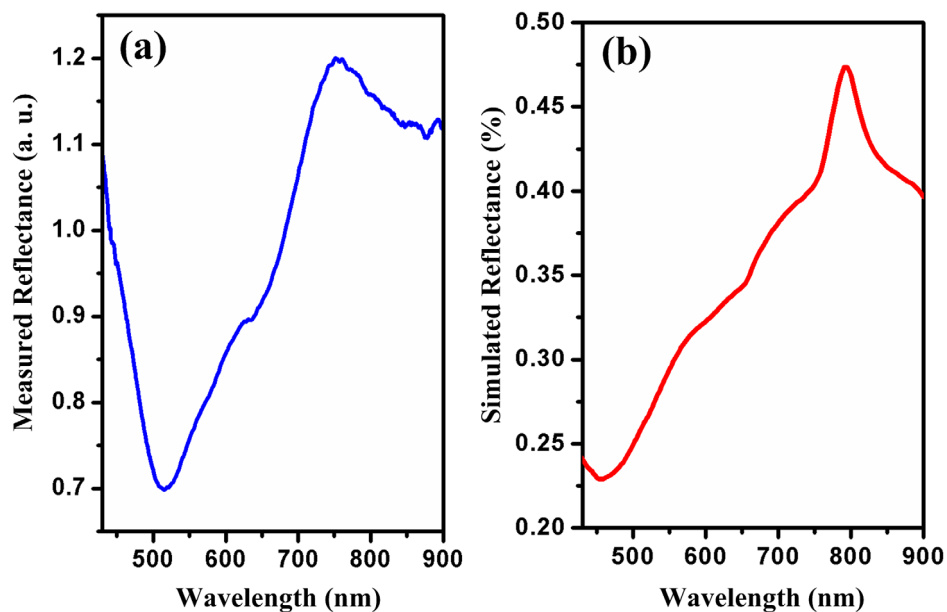
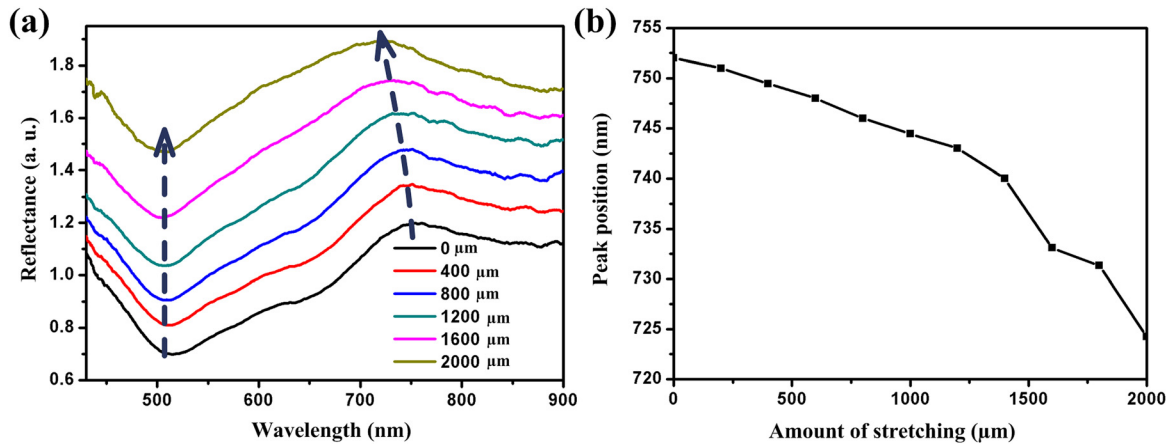


Fig. 4 (a) Measured and (b) FDTD-simulated LSPR reflectance spectrum of the Au nanodisk arrays immobilized on a PDMS substrate in relaxed state



**Fig. 5 (a) Extinction spectra recorded from the Au nanodisk arrays immobilized on a PDMS substrate undergoing various levels of stretching. A blueshift of reflectance peak wavelength is observed. (b) Shift of reflectance peak wavelength as a function of amount of stretch. A tunable reflectance peak shift up to 30 nm is achieved.**

### 3 Results and Discussion

Figure 3(a) shows original microscopic images of a relaxed Au nanodisk array, and a processed image to mark the lattice boundaries of adjacent nanodisks. The arrowed lines denote the three axes of the hexagonally arranged array, and the horizontal line indicates the stretch direction. The maximum stretch is 2000 μm, and the change in period along three axes of the hexagonal array is plotted in Figs. 3(b)–3(d), respectively. The change in period was measured from captured microscopic images and its value was averaged over several locations. We note that only the distance between adjacent nanodisks changed during the stretching process and the shape of the nanodisks maintained the same as in their relaxed state. This is caused by the intermediate PS sphere layer separating the gold nanostructures and the PDMS substrate. The gold nanostructures are stuck to the PS spheres rather than attaching to the PDMS layer directly; thus, the gold structures will not change their shapes unless the stretching force from PDMS substrate is strong enough to tear the PS spheres, which is unlikely to happen in our case.

Upon being stretched, axes 2 and 3 are elongated, while axis 1 is condensed. It can be seen from Fig. 3 that the relation between the stretch amplitude and period shift is nearly linear along all axes. The maximum rate of change of the period along axes 2 and 3 is ~4.3%, and –1.6% for axis 1. Poisson’s ratio ( $\nu$ ) was calculated from the geometric relation between the axes (0.45), which accurately matches the intrinsic material property of PDMS ( $\nu=0.5$ ). Finally, the angle between axes 1 and 2 increases from 60 deg to 62 deg upon maximum stretching, while the angle between axes 2 and 3 decreases to 56 deg.

The LSPR properties of the Au nanodisk arrays, which were immobilized onto the PDMS substrate, were studied by taking the arrays’ reflectance spectrum. Figure 4(a) shows the measured reflectance spectrum of the relaxed Au nanodisk arrays. To further understand the spectrum, a numerical calculation was conducted using commercial software (LUMERICAL FDTD) [58] to simulate a perfect hexagonal array of Au nanodisks standing on a dielectric substrate. The period, the diameter, and the thickness of the Au nanodisks were 1050 nm, 800 nm, and 40 nm, respectively. The dielectric constant of Au was obtained from a fit to the Johnson–Christy data [59]. An unpolarized, broadband light source was set normal to the substrate and the reflectance spectrum is shown in Fig. 4(b) (modeled without Cr adhesion layer).

The reflectance minimum is related to intrinsic absorption and transmission of the incident light by the Au, while the peak indicates minimal coupling between the incident light and the localized surface plasmons. The experiment result closely matched the simulation and confirmed that the tightly packed Au nanoparticle arrays have been formed as expected.

Figure 5(a) shows the reflectance spectra of Au nanodisk arrays on a PDMS substrate undergoing various levels of stretching. The stretching neither broadened nor decreased the intensity of the LSPR spectra. There is no obvious shift in the spectral dip since it represents the intrinsic transmission and absorption of Au and is not dependent on geometry. The reflectance peak, however, exhibits a clear blueshift proportional to the amount of stretch, which is consistent with the observation in Ref. [60]. The reflectance peak shift versus stretch magnitude is plotted in Fig. 5(b); the plot shows a maximum peak shift of 30 nm (from 752 nm in the relaxed state to 722 nm at maximum stretch). The peak shift is reversible, i.e., the peak wavelength moves back to 752 nm when the sample is released, and the tuning of the peak wavelength becomes uniform across the sample. This kind of phenomenon enables the nanodisk array “glued” on a PDMS substrate be used as an ultrasensitive optical tool to monitor small changes of the external tension force applied.

The blueshift of the reflectance peak wavelength is the result of the change in Au nanodisk array geometry. LSPR in nanoparticle arrays is highly dependent on coupling between adjacent particles, which in-turn strongly depends on the interparticle distance. The sample was stretched in only one direction, but due to Poisson’s effect the size in the relaxed direction was decreased while the period in the other two directions was increased. The spacing of the Au nanodisk arrays was not homogeneously changed; however, the effective interparticle distance increased as the sample was stretched, leading to less influence from electron coupling between adjacent Au nanodisks as well as a blueshift in the reflectance peak.

### 4 Conclusions

We have developed a simple, inexpensive method to fabricate patterned Au nanostructures on a PDMS substrate. The plasmonic resonance of the Au nanostructures can be actively controlled by stretching the PDMS substrate. The stretching increases the distance between adjacent Au nanostructures, leading to a shift in their plasmonic resonance. The shift is repeatable, reversible, and has potential applications in LSPR sensing, Raman sensing, and coupled resonance studies.

### Acknowledgment

Yanhui Zhao and Thomas Walker contributed equally to this work. The authors want to thank Dr. Shikuan Yang and Dr. Chenglong Zhao for helpful discussion. This research was supported by NIH Director’s New Innovator Award (1DP2OD007209–01), the National Science Foundation (0824183 and 0801922), U.S. Department of Agriculture (USDA/NRI), Air Force Office of Scientific

Research (AFOSR), and the Penn State Center for Nanoscale Science (MRSEC). Components of this work were conducted at the Penn State node of the NSF-funded National Nanotechnology Infrastructure Network.

## References

- Maier, S. A., 2007, *Plasmonics: Fundamentals and Applications*, Springer, New York.
- Atwater, H. A., 2007, "The Promise of Plasmonics," *Sci. Am.*, **17**, pp. 56–63.
- Ebbesen, T. W., Lezec, H. J., Ghaemi, H. F., Thio, T., and Wolff, P. A., 1997, "Extraordinary Optical Transmission Through Sub-Wavelength Hole Arrays," *Nature*, **391**, pp. 667–669.
- Pendry, J. B., Schurig, D., and Smith, D. R., 2006, "Controlling Electromagnetic Fields," *Science*, **312**, pp. 1780–1782.
- Leonhardt, U., 2006, "Optical Conformal Mapping," *Science*, **312**, pp. 1777–1780.
- Chen, H., Chan, C. T., and Sheng, P., 2010, "Transformation Optics and Metamaterials," *Nature Mater.*, **9**, pp. 387–396.
- Zentgraf, T., Liu, Y., Mikkelsen, M. H., Valentine, J., and Zhang, X., 2011, "Plasmonic Luneburg and Eaton Lenses," *Nat. Nanotechnol.*, **6**, pp. 151–155.
- Gordon, R., 2009, "Proposal for Superfocusing at Visible Wavelengths Using Radiationless Interference of a Plasmonic Array," *Phys. Rev. Lett.*, **102**, p. 207402.
- Zhao, Y., Lin, S. S., Nawaz, A. A., Kiraly, B., Hao, Q., Liu, Y., and Huang, T. J., 2010, "Beam Bending via Plasmonic Lenses," *Opt. Express*, **18**, pp. 23458–23465.
- Si, G., Zhao, Y., Liu, H., Teo, S. L., Zhang, M., Huang, T. J., Danner, A. J., and Teng, J. H., 2011, "Annular Aperture Array Based Color Filter," *Appl. Phys. Lett.*, **99**, p. 033105.
- Fang, N., Lee, H., Sun, C., and Zhang, X., 2005, "Sub-Diffraction-Limited Optical Imaging With a Silver Superlens," *Science*, **308**, pp. 534–537.
- Melville, D. O. S., and Blaikie, R. J., 2005, "Super-Resolution Imaging Through a Planar Silver Layer," *Opt. Express*, **13**, pp. 2127–2134.
- Liu, Z., Lee, H., Xiong, Y., Sun, C., and Zhang, X., 2007, "Far-Field Optical Hyperlens Magnifying Sub-Diffraction-Limited Objects," *Science*, **315**, p. 1686.
- Jacob, Z., Alekseyev, L. V., and Narimanov, E., 2006, "Optical Hyperlens: Far-Field Imaging Beyond Diffraction Limit," *Opt. Express*, **14**, pp. 8247–8256.
- Zhao, Y., Gan, D., Cui, J., Wang, C., Du, C., and Luo, X., 2008, "Super Resolution Imaging by Compensating Oblique Lens With Metallodielectric Films," *Opt. Express*, **16**, pp. 5697–5707.
- Zhao, Y., Nawaz, A. A., Lin, S. S., Hao, Q., Kiraly, B., and Huang, T. J., 2011, "Nanoscale Super-Resolution Imaging via Metal-Dielectric Lens System," *J. Phys. D: Appl. Phys.*, **41**, p. 415101.
- Smalley, J. S. T., Zhao, Y., Nawaz, A. A., Hao, Q., Ma, Y., Khoo, I., and Huang, T. J., 2011, "High Contrast Modulation of Plasmonic Signals Using Nanoscale Dual-Frequency Liquid Crystals," *Opt. Express*, **19**, pp. 15265–15274.
- Hao, Q., Zhao, Y., Juluri, B. K., Kiraly, B., Liou, J., Khoo, I. C., and Huang, T. J., 2011, "Frequency-Addressed Tunable Transmission in Optically Thin Metallic Nanohole Arrays With Dual-Frequency Liquid Crystals," *J. Appl. Phys.*, **109**, p. 084340.
- Liu, Y. J., Zheng, Y. B., Liou, J., Chiang, I., Khoo, I. C., and Huang, T. J., 2011, "All-Optical Modulation of Localized Surface Plasmon Coupling in a Hybrid System Composed of Photo-Switchable Gratings and Au Nanodisk Arrays," *J. Phys. Chem. C*, **115**, pp. 7717–7722.
- Liu, Y. J., Hao, Q., Smalley, J. S. T., Liou, J., Khoo, I. C., and Huang, T. J., 2010, "A Frequency-Addressed Plasmonic Switch Based on Dual-Frequency Liquid Crystal," *Appl. Phys. Lett.*, **97**, p. 091101.
- Liu, Y. J., Zheng, Y. B., Shi, J., Huang, H., Walker, T. R., and Huang, T. J., 2009, "Optically Switchable Gratings Based on Azo-Dye-Doped, Polymer-Dispersed Liquid Crystals," *Opt. Lett.*, **34**, pp. 2351–2353.
- Hsiao, V. K. S., Zheng, Y. B., Juluri, B. K., and Huang, T. J., 2008, "Light-Driven Plasmonic Switches Based on Au Nanodisk Arrays and Photoresponsive Liquid Crystals," *Adv. Mater.*, **20**, pp. 3528–3532.
- Liu, Y. J., Ding, X., Lin, S. S., Shi, J., Chiang, I., and Huang, T. J., 2011, "Surface Acoustic Wave Driven Light Shutters Using Polymer-Dispersed Liquid Crystals," *Adv. Mater.*, **23**, pp. 1656–1659.
- Liu, Y. J., Dai, H. T., Sun, X. W., and Huang, T. J., 2009, "Electrically Switchable Phase-Type Fractal Zone Plates and Fractal Photon Sieves," *Opt. Express*, **17**, pp. 12418–12423.
- Zheng, Y. B., Kiraly, B., Cheunkar, S., Huang, T. J., and Weiss, P., 2011, "Incident-Angle-Modulated Molecular Plasmonic Switches: A Case of Weak Exciton-Plasmon Coupling," *Nano Lett.*, **11**, pp. 2061–2065.
- Zheng, Y. B., Kiraly, B., and Huang, T. J., 2010, "Molecular Machines Drive Smart Drug Delivery," *Nanomedicine*, **5**, pp. 1309–1312.
- Zheng, Y. B., Juluri, B. K., Jensen, L., Ahmed, L., Lu, M., Jensen, L., and Huang, T. J., 2010, "Dynamically Tuning Plasmon-Exciton Coupling in Arrays of Nanodisk-J-Aggregate Complexes," *Adv. Mater.*, **22**, pp. 3603–3607.
- Zheng, Y. B., Hao, Q., Yang, W., Kiraly, B., Chiang, I., and Huang, T. J., 2010, "Light-Driven Artificial Molecular Machines," *J. Nanophotonics*, **4**, p. 042501.
- Juluri, B. K., Lu, M., Zheng, Y. B., Jensen, L., and Huang, T. J., 2009, "Coupling Between Molecular and Plasmonic Resonances: Effect of Molecular Absorbance," *J. Phys. Chem. C*, **113**, pp. 18499–18503.
- Zheng, Y. B., Yang, Y., Jensen, L., Fang, L., Juluri, B. K., Flood, A. H., Weiss, P. S., Stoddart, J. F., and Huang, T. J., 2009, "Active Molecular Plasmonics: Controlling Plasmon Resonances With Molecular Switches," *Nano Lett.*, **9**, pp. 819–825.
- Huang, T. J., 2009, "Recent Developments in Artificial Molecular Machine-Based Active Nanomaterials and Nanosystems," *MRS Bull.*, **33**, pp. 226–231.
- Ye, T., Kumar, A. S., Saha, S., Takami, T., Huang, T. J., Stoddart, J. F., and Weiss, P. S., 2010, "Changing Stations in Single Bistable Rotaxane Molecules Under Electrochemical Control," *ACS Nano*, **4**, pp. 3697–3701.
- Li, D., Baughman, R. H., Huang, T. J., Stoddart, J. F., and Weiss, P. S., 2009, "Molecular, Supramolecular, and Macromolecular Motors and Artificial Muscles," *MRS Bull.*, **34**, pp. 671–681.
- Huang, T. J., Brough, B., Ho, C., Liu, Y., Flood, A. H., Bonvallet, P. A., Stoddart, J. F., Baller, M., and Maganov, S., 2004, "A Nanomechanical Device Based on Linear Molecular Motors," *Appl. Phys. Lett.*, **85**, pp. 5391–5393.
- Srituravanich, W., Pan, L., Wang, Y., Sun, C., Bogy, D. B., and Zhang, X., 2008, "Flying Plasmonic Lens in the Near Field for High-Speed Nanolithography," *Nat. Nanotechnol.*, **3**, pp. 733–737.
- Juluri, B. K., Chaturvedi, N., Hao, Q., Lu, M., Velego, D., Jensen, L., and Huang, T. J., 2011, "Scalable Manufacturing of Plasmonic Nanodisk Dimers and Cups Nanostructures Using Salting-Out Quenching Method and Colloidal Lithography," *ACS Nano*, **5**, pp. 5838–5847.
- Hao, Q., Zeng, Y., Juluri, B. K., Wang, X., Kiraly, B., Chiang, I., Jensen, L., Werner, D. H., Crespi, V., and Huang, T. J., 2011, "Metallic Membranes With Subwavelength Complementary Patterns: Distinct Substrates for Surface Enhanced Raman Scattering," *ACS Nano*, **5**, pp. 5472–5477.
- Hao, Q., Zeng, Y., Wang, X., Zhao, Y., Wang, B., Chiang, I., Werner, D. H., Crespi, V., and Huang, T. J., 2010, "Characterization of Complementary Patterned Metallic Membranes Produced Simultaneously by a Dual Fabrication Process," *Appl. Phys. Lett.*, **97**, p. 193101.
- Zheng, Y. B., Juluri, B. K., Kiraly, B., and Huang, T. J., 2010, "Ordered Au Nanodisk and Nanohole Arrays: Fabrication and Applications," *ASME J. Nanotechnol. Eng. Med.*, **1**, p. 031011.
- Hutter, E., and Fendler, J. H., 2004, "Exploitation of Localized Surface Plasmon Resonance," *Adv. Mater.*, **16**, pp. 1685–1706.
- Willets, K. A., and Van Duyne, R. P., 2007, "Localized Surface Plasmon Resonance Spectroscopy and Sensing," *Annu. Rev. Phys. Chem.*, **58**, pp. 267–297.
- Wiley, B., Sun, Y. G., Chen, J. Y., Cang, H., Li, Z. Y., Li, X. D., and Xia, Y. N., 2005, "Shape-Controlled Synthesis of Silver and Gold Nanostructures," *MRS Bull.*, **30**, pp. 356–361.
- Xia, Y. N., and Halas, N., 2005, "Shape-Controlled Synthesis and Surface Plasmonic Properties of Metallic Nanostructures," *MRS Bull.*, **30**, pp. 338–348.
- Murray, W. A., Suckling, J. R., and Barnes, W. L., 2006, "Overlayers on Silver Nanotriangles: Field Confinement and Spectral Position of Localized Surface Plasmon Resonances," *Nano Lett.*, **6**, pp. 1772–1777.
- Sun, Y. G., and Xia, Y. N., 2002, "Shape-Controlled Synthesis of Gold and Silver Nanoparticles," *Science*, **298**, pp. 2176–2179.
- Wang, H., Brandl, D. W., Le, F., Nordlander, P., and Halas, N. J., 2006, "Nanorice: A Hybrid Plasmonic Nanostructure," *Nano Lett.*, **6**, pp. 827–832.
- Wang, H., Brandl, D. W., Nordlander, P., and Halas, N. J., 2007, "Plasmonic Nanostructures: Artificial Molecules," *Acc. Chem. Res.*, **40**, pp. 53–62.
- Yonzon, C. R., Stuart, D. A., Zhang, X. Y., McFarland, A. D., Haynes, C. L., and Van Duyne, R. P., 2005, "Towards Advanced Chemical and Biological Nanosensors—An Overview," *Talanta*, **67**, pp. 438–448.
- Zheng, Y. B., Jensen, L., Yan, W., Walker, T. R., Juluri, B. K., Jensen, L., Huang, T. J., 2009, "Chemically Tuning the Localized Surface Plasmon Resonances of Gold Nanostructure Arrays," *J. Phys. Chem. C*, **113**, pp. 7019–7024.
- Juluri, B. K., Zheng, Y. B., Ahmed, D., Jensen, L., and Huang, T. J., 2008, "Effects of Geometry and Composition on Charge-Induced Plasmonic Shifts in Gold Nanoparticles," *J. Phys. Chem. C*, **112**, pp. 7309–7312.
- Zheng, Y. B., Juluri, B. K., Mao, X., Walker, T. R., and Huang, T. J., 2008, "Systematic Investigation of Localized Surface Plasmon Resonance of Long-Range Ordered Au Nanodisk Arrays," *J. Appl. Phys.*, **103**, p. 014308.
- Zheng, Y. B., Huang, T. J., Desai, A. Y., Wang, S. J., Tan, L. K., Gao, H., and Huan, A. C. H., 2007, "Thermal Behavior of Localized Surface Plasmon Resonance of Au/TiO<sub>2</sub> Core/Shell Nanoparticle Arrays," *Appl. Phys. Lett.*, **90**, p. 183117.
- Krasavin, A. V., and Zheludev, N. I., 2004, "Active Plasmonics: Controlling Signals in Au/Ga Waveguide Using Nanoscale Structural Transformations," *Appl. Phys. Lett.*, **84**, pp. 1416–1418.
- MacDonald, K. F., Samson, Z. L., Stockman, M. I., and Zheludev, N. I., 2009, "Ultrafast Active Plasmonics," *Nat. Photonics*, **3**, pp. 55–58.
- Liu, Y. J., Shi, J., Zhang, F., Liang, H., Xu, J., Lakhtakia, A., Fonash, S. J., and Huang, T. J., 2011, "High-Speed Optical Lumidity Sensors Based on Chiral Sculptured Thin Film," *Sens. Actuators B*, **156**, pp. 593–598.
- Zhang, B., Zhao, Y., Hao, Q., Kiraly, B., Khoo, I., Chen, S., and Huang, T. J., 2011, "Polarization Independent Dual Band Infrared Perfect Absorber Based on a Metal-Dielectric-Metal Elliptical Nanodisk Array," *Opt. Express*, **19**, pp. 15221–15228.
- Chen, X., Lenhart, S., Hirtz, M., Lu, N., Fuchs, H., and Chi, L., 2007, "Langmuir-Blodgett Patterning: A Bottom-Up Way to Build Mesostructures Over Large Areas," *Acc. Chem. Res.*, **40**, pp. 393–401.
- Lumerical FDTD Solution, ver 7.5, 2011, <http://www.lumerical.com/>
- Johnson, P. B., and Christy, R. W., 1972, "Optical Constants of the Nobel Metals," *Phys. Rev. B*, **6**, pp. 4370–4379.
- Yang, S. K., Cai, W. P., Kong, L. C., and Lei, Y., 2010, "Surface Nanometer-Scale Patterning in Realizing Large-Scale Ordered Arrays of Metallic Nanoshells With Well-Defined Structures and Controllable Properties," *Adv. Funct. Mater.*, **20**, pp. 2527–2533.